Statistical Optimization of Production Conditions of Polycaprolactone-Chitosan-Curcumin Particles

Marjan Roshandel[1], Rahmat Sotudeh-Gharebagh*[1], Sasan Mirzakhanlouei[2], Reza Hajiaghaee[2] and Reza Ghaffarzadegan[2]

1. School of Chemical Engineering, College of Engineering, University of Tehran, Tehran, Iran
2. Department of Pharmacognosy and Pharmaceutics, Institute of Medicinal Plants, ACECR, Karaj, Iran

(Received: 07/28/2018, Revised: 08/19/2018, Accepted: 09/08/2018)
[DOI: 10.22059/JCHPE.2018.262918.1240]

Abstract

Curcumin is an herbal plant with great therapeutic applications. Although it is useful in treating several diseases, its low solubility in water and low bioavailability in living systems are limiting factors in using curcumin as a medicine. One way to overcome these shortcomings is the production of curcumin micro/nanoparticles. In this research, the particles of curcumin loaded with polycaprolactone (PCL)/chitosan were synthesized by the electrospray technique. To obtain the optimal conditions, statistical optimization was carried out through the Response Surface Method (RSM). The effects of flow rate, polymer concentration, and PCL weight percentage on solution properties, mean particle size, and particle size distribution were investigated. According to experimental results, the optimal size (471 nm) and size distribution (103) of particles were found at the lowest level of polymer concentration (2%) and flow rate (0.25 ml/hr) and the highest level of PCL weight percentage (80%). Thus, the result of this study can be used to improve the quality of curcumin based medicine.

Keywords

Curcumin;
Design of Experiment;
Electrospray;
Micro/Nano Particles;
Statistical Optimization

1. Introduction

Nowadays, cancer causes a high mortality rate around the world as it rapidly destroys healthy tissues. Various therapies for this disease have been reported in the literature; however, none of them completely eliminates tumors or prevents their distribution within human tissues. Chemotherapy, radiation therapy and surgery are the conventional treatment methods used for decades around the world bringing some success in cancerous cell destruction. However, their side effects have raised considerable debate among scientists [1]. The introduction of nanotechnology into the novel pharmaceutical formulation during the last decade has led to promising results in cancer treatment [2]. Development of nanoparticulate drugs, with controlled release patterns, offers chances to overcome this tedious disease. The combined application of herbal-based nano-materials with a prop-

* Corresponding Author.
Tel.: +98 21 66967781
Email: sotudeh@ut.ac.ir (R. Sotudeh-Gharebagh)

er formulation can minimize drug side effects in terms of toxicity for normal tissues [3].

Several herbal materials were proposed to treat cancerous cells and prevent further growth. Among them, curcumin, as a polyphenol and the active component of Turmeric shows promising results. In 1815, curcumin was first extracted from rhizome of *Turmeric* by Vogel et al. [4]. In 1870, it was obtained in crystalline form for the first time [5]. In 1910, Lampe et al. [6] confirmed and synthesized Feruloylmethane skeleton. Curcumin has miscellaneous therapeutic effects such as anti-oxidant [3, 7-9], anti-inflammatory [10-12], anti-thrombotic[9], cardiovascular protective [13-15] and anti-cancer [3, 16-18]. However, its low solubility in water and low bioavailability are the limiting factors against its utilization in novel pharmaceutical applications [19, 20].

Different approaches have been reported in the literature to resolve these drawbacks. In recent years, the production of polymeric particles containing curcumin was successfully achieved [1]. With this approach, the particle size is reduced and at the same time, the specific surface of particles is increased, which in turn causes increasing their solubility in water and bioavailability. This leads to the delivery of more concentrated therapeutic agents to target tissues, improving efficiency, increasing the stability of the drug, and preventing its chemical decomposition [21].

Since the size, morphology and size distribution of drug carriers affect drug release pattern in the body, selection of an appropriate process and operating conditions has a major impact on the quality of final products. There are a variety of techniques for the synthesis of nanoparticles such as nanoprecipitation, emulsification/solvent diffusion, salting out, supercritical fluid technology and electrospray [21]. Among these, electrospray has gained special attention in the last few years due to the production of particles in micro and nano size, narrow size distribution and one step processing [22-26]. To reach the optimum process conditions, statistical optimization is used considering all leading factors.

In the electrospray technique, particles are generated by applying a strong electrical field over a polymeric solution. The liquid flow pattern in a syringe connected to a needle is altered by the electrical field, which causes the elongation of the liquid and forming a jet. Thereafter, the solvent is evaporated on its way from the needle to a collector where particles are collected [27-30]. Experimental set-up, polymer type, concentration and molecular weight, solvent properties, voltage, flow rate, temperature, pressure, humidity, needle-to-collector distance, needle size and drug/polymer ratio are the effective parameters of this process [31-33]. There are some studies which considered the effects of different parameters on size and size distribution of fabricated particles [29, 33-35]; nevertheless, to the best of the authors' knowledge, there are limited studies related to the statistical optimization of the electrospray process [36].

In this study, statistical optimization was conducted on the synthesis of polymeric particles of curcumin by electrospray. Polycaprolactone and chitosan were the utilized polymers. There are some studies which used these polymers together in synthesizing micro and nanoparticles and fibers [37-39]. Polycaprolactone is non-toxic, biodegradable and approved by Food and Drug Administration (FDA). As it is hydrophobe, synthesis of micro/nano particles by using pure polycaprolactone is so complicated due to the agglomeration of particles [40]. To prevent the agglomeration phenomena, complex molecules such as polysaccharides can be used. Chitosan is a cationic polysaccharide, non-toxic, biocompatible, hydrophile, biodegradable and soft-tissue compatible material [41,42]. Since chitosan has too many active cations, its addition to a solution increases its conductivity and viscosity and enhances the particle size. However, since chitosan has so many functional groups, it forms hydrogen bonds, which leads to folding and preventing fiber formation [43].

The objective of this study is to identify the optimal process conditions for synthesizing PCL-chitosan-curcumin micro/nano particles by conducting statistical optimization. In addition, statistical models were proposed to investigate interactions among parameters and their effects on particle size and size distribution.

2. Materials and Methods

2.1. Materials

Curcumin (analytical standard grade, Mw=368.38 kg/kmol), polycaprolactone (average Mn=80000) and chitosan (deacetylation degree 80%, viscosity

200 cP) were purchased from Sigma-Aldrich (USA). Acetic acid was supplied from Merck (Germany).

2.2. Methods

2.2.1. Experimental design

Design of Experiment (DOE) was used for solutions preparation and particles synthesis using Minitab 16©. The DOE was carried out by Response Surface Methods (RSM), central composite-face centered. The RSM is used to examine the relationship between one or more response variables and a set of quantitative experimental variables or factors. This method is often employed when a few controllable factors are identified and factors settings which optimize the response are needed. Based on pretest results, polymer concentration, PCL weight percentage, and flow rate had significant effects on particle size and particle size distribution. Accordingly, these three factors were chosen as independent parameters and subsequently, three levels were defined for each parameter again based on the pretests. Tables 1 and 2 tabulate the independent and constant parameters with their levels, respectively. Level for each constant factor was evaluated according to the pretest results. Based on the method and number of independent factors, the number of experiments which Minitab defined was 20, including 14 cube points and 6 center points. Table 3 tabulates coded value of each independent variable and amount of each dependent variable per each run.

2.2.2. Solution preparation

Based on DOE and levels of the independent parameters (Tables 1 and 2), the required amounts of polymers were weighted for each solution and then the weight of curcumin was determined to be 10% of polymer weight. Polymeric solutions were prepared by dissolving the materials in acetic acid 90% (v/v). The solvent was chosen due to the complete solubility of all three materials, sufficient evaporation of the solvent during the process, non-forming fibers and the appropriate size of the fabricated particles. These claims were determined through pretests. In order to obtain a comprehensive mixture and limpid solutions, each solution was stirred for 20 h at ambient temperature (25-30 °C) and pressure of 0.8 atm then sonicated for 1 h. Thereafter, solutions were stored in bottles and needles to conduct analyses and produce micro/nano particles.

2.2.3. Viscosity measurement

Viscosity was measured according to ASTM D445 method at 30 °C with Stanhope-Seta (made in England). Table 3 tabulates the viscosity results for all samples.

2.2.4. Surface tension measurement

The surface tension of samples was measured by the ring method using a Krüss K100 Processor Tensiometer (made in Germany). For each sample, 10 measurements were carried out with 1 min intervals and then the mean value was reported. Table 3 shows the surface tension results for all samples.

2.2.5. Electrical conductivity measurement

Electrical conductivity was measured for each sample using a digital conductometer (Data line conductivity-meter WinLab Windaus No: 1525032 made in Germany) at ambient temperature. The electrical conductivity results for all samples are presented in Table 3.

2.2.6. Electrospray process

In order to produce curcumin containing micro/nano particles, the solution was loaded into a 1 ml plastic syringe with a 24-gauge blunt-end stainless steel needle. Syringe Pump (JSM 1600) was used for controlled injection of the solution. A constant voltage of 18 kV was used as the driving force for the jet formation and a tip to collector distance of 15 cm was chosen as the optimized distance for solvent evaporation. The samples were collected on a conductive aluminum foil, ready for the analyses. Fig. 1 shows the setup used in this study.

Table 1. Independent parameters of the process

Independent parameters	Symbol	Levels		
		-1	0	1
Polymer's concentration % (polymers weight/solutions volume)	A	2	2.5	3
% PCL (PCL weight/total polymer weight)	B	60	70	80
Flow (ml/h)	C	0.25	0.5	0.75

Table 2. Constant parameters of the process

Temperature (°C)	Pressure (atm)	Curcumin concentration* (%)	Voltage (kV)	Needle size (gauge)	Tip to the collector distance (cm)
25-30	0.8	10	18	24	15

*curcumin weight/polymer weight

Table 3. RSM Central composite-face centered experimental design with 20 runs and the corresponding responses

Run #	Independent variables (coded value)			Dependent variables				
	A	B	C	Y_1(viscosity) cSt	Y_2(electrical conductivity) µs	Y_3(size) nm	Y_4(size distribution)	Y_5(surface tension) mN/m
1	-1	-1	-1	18.54	135	626	295	27.40
2	+1	-1	-1	61.69	201	752	430	27.70
3	-1	+1	-1	14.73	71	471	103	28.10
4	+1	+1	-1	37.54	100	492	192	27.80
5	-1	-1	+1	19.87	141	704	421	28.80
6	+1	-1	+1	63.76	206	803	681	27.65
7	-1	+1	+1	15.10	83	615	356	28.30
8	+1	+1	+1	38.30	104	850	781	29.25
9	-1	0	0	17.38	105	990	589	28.90
10	+1	0	0	49.87	148	1226	841	29.40
11	0	-1	0	32.63	170	936	729	28.20
12	0	+1	0	22.69	91	609	289	27.45
13	0	0	-1	26.50	118	526	202	29.10
14	0	0	+1	27.10	120	586	409	28.85
15	0	0	0	28.07	131	692	461	27.78
16	0	0	0	30.98	140	791	611	28.05
17	0	0	0	29.45	136	751	588	27.89
18	0	0	0	31.50	144	811	510	27.63
19	0	0	0	27.76	125	668	544	27.10
20	0	0	0	28.98	134	721	422	27.15

2.2.7. Field emission scanning electron microscope (FE-SEM)

Size distribution, size, and morphology of particles were characterized using Field Emission Scanning Electron Microscopic (Hitachi S4160). Samples were coated with a thin layer of gold and then analyzed with FE-SEM. For each sample, the diameter of 300 particles was measured using Image-J software (version 1.48, Wayne Rasband, NIH, USA). Thereafter, the mean and standard deviation values were calculated for each sample as indicators for particle size and size distribution, respectively. Table 3 shows the FE-SEM results for all samples. One image per each run is shown in Fig. 2.

2.2.8. Fourier transform infrared spectroscopy (FTIR)

FTIR was used for chemical analysis of the produced particles using Perkin Elmer FT-IR Spectrometer Spectrum Two (made in USA).

3. Results and Discussion

In order to analyze the experimental results, five parameters, including solution viscosity, electrical conductivity, and surface tension, particle size, and particle size distribution) were designated as dependent variables. Model fitting was used to assess the effects of the independent parameters on each process response then statistical optimization was conducted to predict the optimized conditions to produce particles with the smallest size and lowest size distribution.

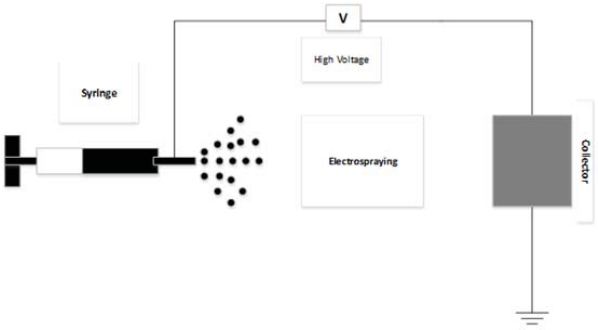

Figure 1. The setup used in this study

3.1. Model fitting

To recognize significant parameters and fit a model, analysis of variance (ANOVA) test was applied to each dependent variable. Table 4 tabulates a summary of the results obtained from the test.

A p-value lower than 0.05 for an independent variable indicates that the variable had a significant effect on the defined dependent variable. Therefore, the model defined for each dependent variable includes all significant parameters.

The criteria for precision and accuracy of a model are p-value of lack of fit and R^2 as well as R^2_{adj}, respectively. When p-value of lack of fit is greater than 0.05, it means that the predictive model has enough precision. R^2 and R^2_{adj} should be higher than 70% for a model in order to confirm its accuracy for prediction of the dependent variable.

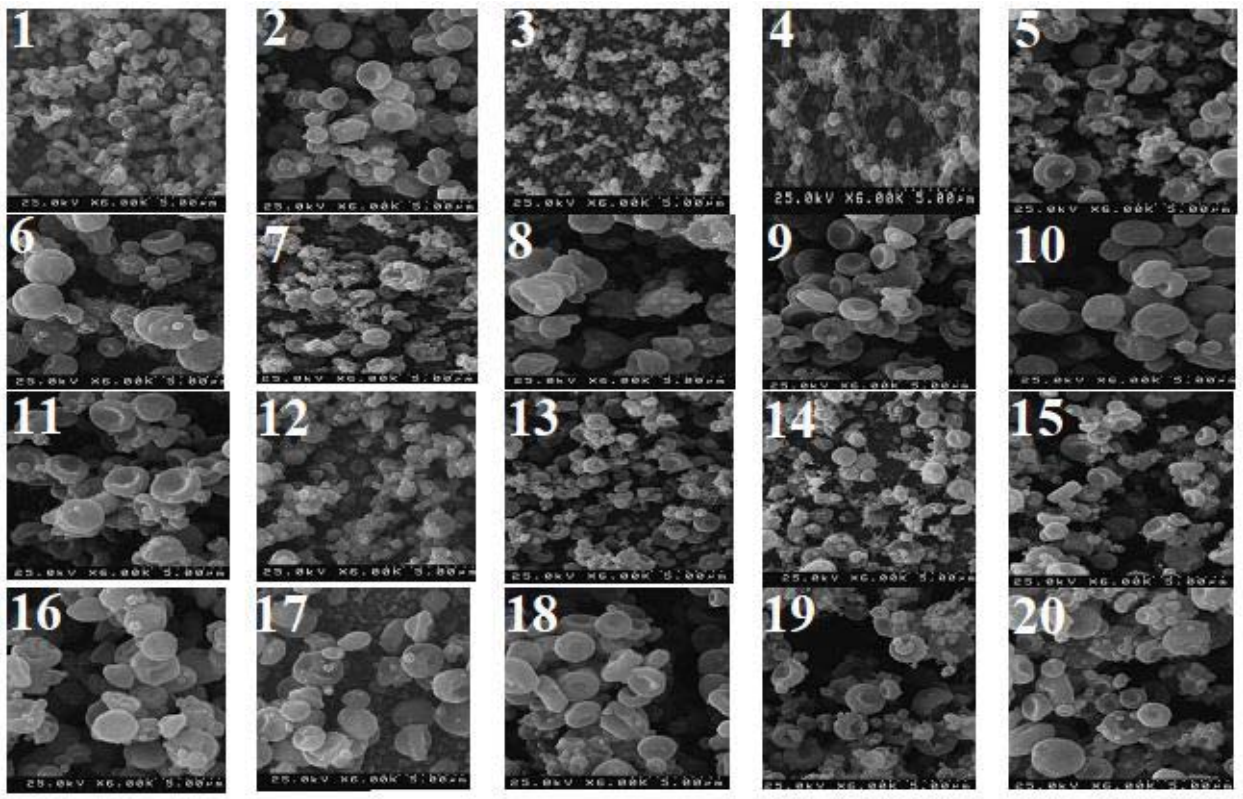

Figure 2. FE-SEM images for all samples

Table. 4 Table of ANOVA, Coefficient and p-value for dependent variables

Term	Viscosity		Electrical conductivity		Size		Size distribution	
	Coeff.	p-value	Coeff.	p-value	Coeff.	p-value	Coeff.	p-value
Constant	28.7833	0.000	131.417	0.000	781.677	0.000	533.87	0.000
A	16.4660	0.000	22.340	0.000	71.697	0.036	116.23	0.003
B	-6.7250	0.000	-40.500	0.000	-78.405	0.024	-83.79	0.017
C	0.6010	0.291	2.896	0.213	69.160	0.042	142.84	0.001
A*A	5.8518	0.000	0.634	0.882	262.117	0.001	164.42	0.014
B*B	-0.1132	0.915	3.934	0.366	-73.530	0.222	-41.88	0.469
C*C	-0.9732	0.367	-7.046	0.121	-290.02	0.000	-245.13	0.001
A*B	-5.2387	0.000	-10.100	0.002	3.866	0.909	15.11	0.653
A*C	0.0313	0.960	-1.175	0.640	23.387	0.496	57.51	0.108
B*C	-0.1738	0.779	0.650	0.795	46.637	0.190	58.41	0.104
Lack of fit	-	0.327	-	0.411	-	0.059	-	0.204
R^2	99.18%	-	97.93%	-	85.78%	-	88.99%	-
R^2_{adj}	98.44%	-	96.06%	-	72.99%	-	79.08%	-

3.1.1. Solution viscosity

The predicted model for solution viscosity is:

$$Y_1 = 16466A - 6.725B + 5.8516\ A*A - 5.2387\ A*B + 28.7833 \quad (1)$$

Eq. 1 shows that polymer concentration, %PCL, square of polymer concentration, and the interaction between polymer concentration and % PCL have a significant effect on the solution viscosity.

Fig. 3 shows the effect of chitosan weight on the viscosity of the solution. Based on Fig. 3, for all 3 levels of polymer concentration, increasing chitosan weight enhances the viscosity of the solution (it is also reported by Van der Schueren et al. [39]). Among all levels of polymer concentration with constant chitosan weight, the viscosity increased at higher concentration of polymer due to the higher amounts of PCL in the solution.

In samples with constant parameter A (e.g. samples 2 and 4), the sample with higher %PCL (i.e. lower chitosan's weight) had lower viscosity. Increasing polymer concentration led to an increase in viscosity and size of particles (e.g. samples 1 and 2). The sample with the lowest viscosity (sample 4) had the smallest size.

3.1.2. Solution electrical conductivity

The predicted model for solution electrical conductivity is:

$$Y_2 = 22.34A - 40.5B - 10.1\ A*B + 131.417 \quad (2)$$

Eq. 2 shows that polymer concentration, %PCL, and the interaction between polymer concentration and %PCL had a significant effect on the electrical conductivity of the solution.

Fig. 4 shows the effect of chitosan weight on the electrical conductivity of the solution. Based on Fig. 4, for all three levels of polymer concentration, by increasing chitosan weight, the electrical conductivity of the solution increased, which is due to the active cations of chitosan. Moreover, among samples with equal polymer concentration (e.g. samples 1 and 3), the one with more chitosan content had higher electrical conductivity with larger particles. Graphs of different levels of polymer concentration were close to each other since PCL did not have a significant effect on the electrical conductivity of the solution (it is also reported by Van der Schueren et al. [39]) therefore samples with similar chitosan weight (e.g. samples 4 and 9) have similar electrical conductivity.

3.1.3. Solution surface tension

As it is reported in Table 3, all samples had similar surface tension values. The reason is that the same solvent was used for all samples and the polymer concentration did not have a significant effect on the surface tension, therefore, model fitting for the solution surface tension did not accomplish.

3.1.4. Particle size

The predicted model for particle size is:

$$Y3 = 71.697\ A - 78.405\ B + 69.16\ C + 262.117\ A*A - 290.021\ C*C + 781.667 \quad (3)$$

Eq. 3 shows that polymer concentration, %PCL, flow rate, square effect of polymer concentration, and square effect of flow rate had a significant effect on the size of the synthesized particles. Fig. 5 shows the effect of %PCL and flow rate on the size of synthesized particles under constant polymer concentration (%2.5).The following equations are suggested by Hartman et al. and Ganan-Calvo [44, 45] for the electrospray process.

$$d=\alpha((\rho Q^4\varepsilon_0)/I^2)^{1/6} \quad (4)$$

$$I\approx(\gamma KQ)^{1/2} \quad (5)$$

where d is the particle diameter, α is a constant, ε_0 is the permittivity of vacuum, K is the liquid conductivity, I is the current, Q is the flow rate and γ is the surface tension in ambient. As it is shown in the equations, higher flow rate results in the enhanced diameter of particles. Therefore, there is an agreement between the outcomes of the current study and this fact, which is shown in Fig. 5. In this study, by increasing the flow rate up to 0.6 ml/h, the particle diameter increased; however, it decreased beyond this point that could be due to voltage instability. In such conditions, The Taylor cone and consequently, the conditions and results of the process will also be unstable. In our study, voltage was considered as a constant parameter and it seems that it was not stable for all conditions.

By increasing the weight of PCL (i.e. decreasing chitosan weight), the viscosity and electrical conductivity of the solution and the particle diameter were decreased [39] (it is shown by the x axis in Fig. 5). There is a contradiction in the literature in terms of the effect of electrical conductivity on particle diameter. Some studies reported that decreasing the electrical conductivity of the solution decreases particle diameter [46], while others reported an increase [47]. In the current study, adding more chitosan conduced increasing the electrical conductivity and consequently, the particle diameter was increased.

3.1.5. Particle size distribution

The predicted model for particle size distribution is:

$$Y4 = 115.22\ A - 82.78\ B + 141.83\ C + 164.87\ A*A - 244.68\ C*C + 533.68 \quad (6)$$

Eq. 6 shows that polymer concentration, %PCL, flow rate, square effect of polymer concentration, and square effect of flow rate had a significant effect on the particle size distribution. Fig. 6 shows the effect of %PCL and flow rate on the size distribution of the synthesized particles under constant polymer concentration (%2.5).

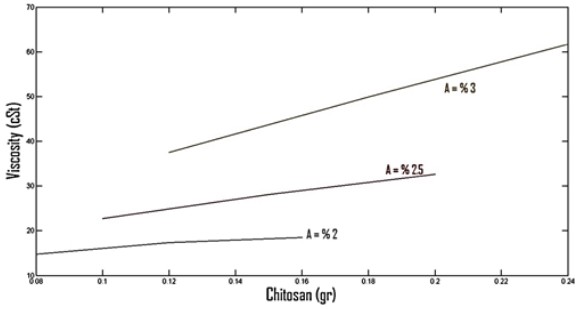

Figure 3. Effect of chitosan weight on the viscosity of the solution

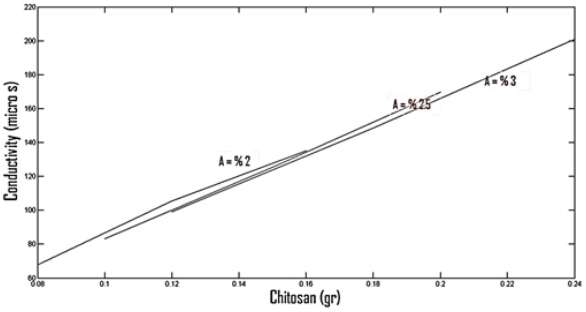

Figure 4. Effect of chitosan weight on the electrical conductivity of solution

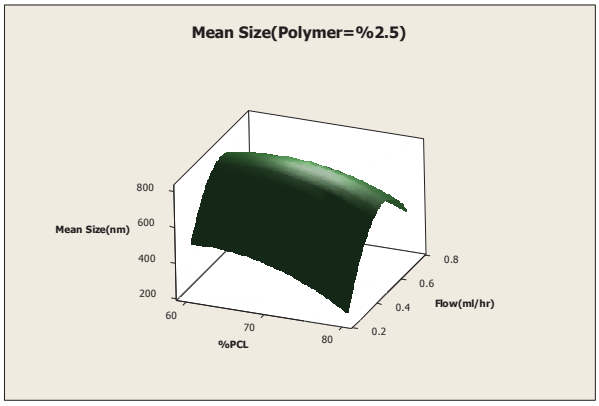

Figure 5. Effect of %PCL and flow rate on the size of the synthesized particles under constant polymer concentration (%2.5)

By increasing the flow rate, the size distribution was increased as well. Voltage was stable for size

distribution (it is shown by y axis in Fig. 6). By increasing the weight of PCL (i.e. decreasing the weight of chitosan), the solution viscosity was reduced; thus, the particle size distribution was reduced, too.

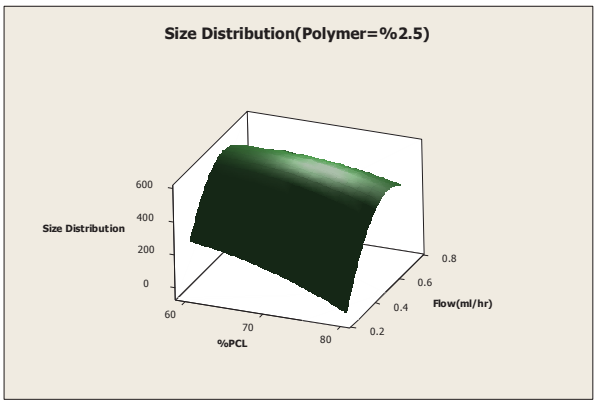

Figure 6. Effect of %PCL and flow rate on the size distribution of the synthesized particles under constant polymer concentration (%2.5)

3.2. Optimization

Using Minitab and analyzing responses, the optimum conditions for the process were achieved, which was found to be 2.18%, 80% and 0.3 ml/hr for polymer concentration, %PCL, and flow rate, respectively. In order to validate the results, the optimum sample was synthesized for 3 times. Table 5 shows the dependent variables for the optimum samples. The optimum conditions were expected to provide the smallest particle size and particle size distribution for the synthesized particles. As it is reported in Table 5, the three optimum samples had a similar particle size and the particle size distribution which confirmed the precision of the experiments. Fig. 7 shows FE-SEM images of the optimum samples.

3.3. Fourier transform infrared spectroscopy for the optimum sample

In order to prove the existence of curcumin and both polymers in the synthesized samples, FTIR was carried out on the optimized samples. Fig. 8 shows the FTIR graphs.

From top to bottom, each graph is related to PCL, optimum sample, curcumin, and chitosan, respectively. For curcumin the bands at 3200-3600 cm^{-1}, 2850-3000 cm^{-1}, 1670-1820 cm^{-1}, 1400-1600 cm^{-1} and 1000-1300 cm^{-1} indicate OH, C-H, C=O, C=C and C-O bonding, respectively [48]. Presence of these peak values and lack of the bands related to impure curcumin in its graph proves the purity of curcumin. Characteristic bands for PCL are 2850-3000 cm^{-1}, 1670-1820 cm^{-1} and 1000-1300 cm^{-1} that indicate C-H, C=O and C-O bonding, respectively [49]. Presence of these peaks in the graph of PCL proves the purity of PCL as well. For chitosan the bands at 3200-3600 cm^{-1}, 3100-3500 cm^{-1}, 2850-3000 cm^{-1} and 1670-1820 cm^{-1} indicate OH, NH_2, C-H and C-O bonding, respectively [50]. Presence of these peaks in the graph of chitosan proves the purity of chitosan. Finally, presence of similar peaks in the graph of the optimum sample proves the presence of these materials in the synthesized samples.

Table 5. Dependent variable for the optimum samples

Sample#	Size (nm)	Size distribution	Viscosity (cSt)	Electrical conductivity (μs)	Surface tension (mN/m)
1	430	104	15.35	72.5	27.54
2	438	104	15.8	73.8	27.3
3	455	106	16.35	75.6	27.2

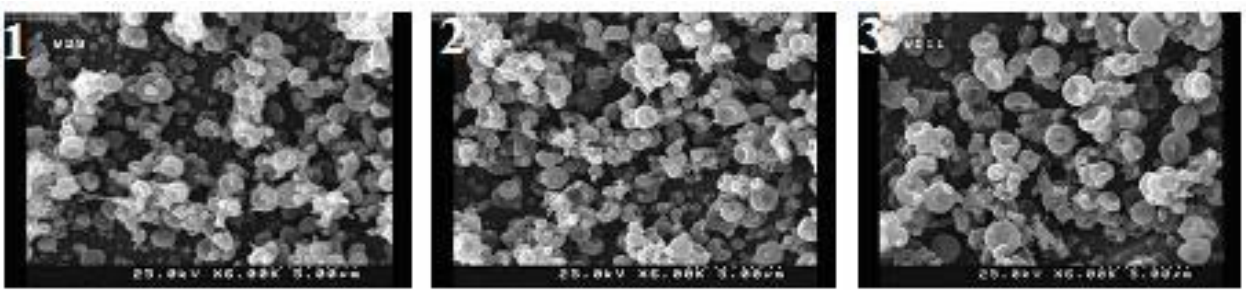

Figure 7. FE-SEM of the optimized samples.

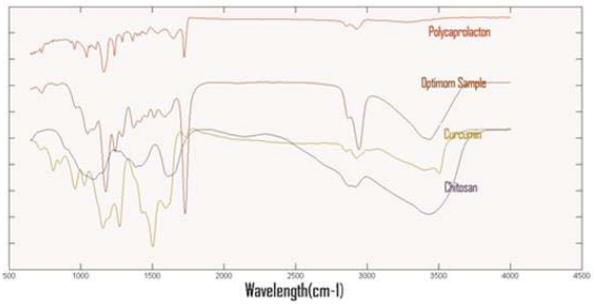

Figure 8. Graphs of FTIR

4. Conclusions

Purpose of this study was to statistically optimize the synthesis of curcumin micro/nano particles by using the electrospray technique. Effects of three independent parameters (flow rate, polymer concentration, and %PCL) were assessed on particle size and size distribution in order to predict conditions for synthesis of the smallest size and lowest size distribution of curcumin micro/nano particles. Both the smallest particle size and lowest particle size distribution were achieved at the lowest level of polymer concentration and flow rate while %PCL was at the highest level. Validation of optimization was performed by replicating the synthesis of the optimum sample for three times. Finally, FTIR test confirmed the existence of curcumin and both polymers in the optimum samples. Synthesized these particles will expand using curcumin in the pharmaceutical industry according to results obtained from statistical optimization and FTIR test.

References

[1] Yallapu, M.M., Jaggi, M. and Chauhan, S. C. (2012). "Curcumin nanoformulations: a future nanomedicine for cancer." *Drug Discovery Today*, Vol. 17, No. 1-2, pp. 71-80.

[2] Misra, R., Acharya, S. and Sahoo, S. K. (2010). "Cancer nanotechnology: application of nanotechnology in cancer therapy." *Drug Discovery Today*, Vol. 15, No. 19-20, pp. 842-850.

[3] Maheshwari, R. K., Singh, A.K., Gaddipati, J. and Srimal, R. C. (2006). "Multiple biological activities of curcumin:" a short review. *Life Sciences*, Vol. 78, No. 18, pp. 2081-2087.

[4] Vogel, H. A. and Pelletier, J. (1815). "Curcumin-biological and medicinal properties." *J Pharma*, Vol. 2, No. 50, p. 24.

[5] Menon, V. P. and Sudheer, A. R. (2007). Antioxidant and anti-inflammatory properties of curcumin, "*The molecular targets and therapeutic uses of curcumin in health and disease*." Vol. 595, pp. 105-125. Springer. Boston.

[6] Goel, A., Kunnumakkara, A. B. and Aggarwal, B.B. (2008). "Curcumin as "Curecumin": from kitchen to clinic." *Biochemical Pharmacology*, Vol. 75, No. 4, pp. 787-809.

[7] Masuda, T., Maekawa, T., Hidaka, K., Bando, H. Takeda, Y., and Yamaguchi, H. (2001). "Chemical studies on antioxidant mechanism of curcumin: analysis of oxidative coupling products from curcumin and linoleate." *Journal of Agricultural and Food Chemistry*, Vol. 49, No. 5, pp. 2539-2547.

[8] Miquel, J., Bernd, A., Sempere, J. M., Dıaz-Alperi, J. And Ramırez, A. (2002). "The curcuma antioxidants: pharmacological effects and prospects for future clinical use. A review." *Archives of Gerontology and Geriatrics*, Vol. 34, No. 1, pp. 37-46.

[9] Kikuchi, H., Kuribayashi, F., Kiwaki, N. and Nakayama, T. (2010). "Curcumin dramatically enhances retinoic acid-induced superoxide generating activity via accumulation of p47-phox and p67-phox proteins in U937 cells." *Biochemical and Biophysical Research Communications*, Vol. 395, No. 1, pp. 61-65.

[10] Srimal, R. C. and Dhawan, B. N. (1973). "Pharmacology of diferuloyl methane (curcumin), a non-steroidal anti-inflammatory agent." *Journal of Pharmacy and Pharmacology*, Vol. 25, No. 6, pp. 447-452.

[11] Agarwal, B. B. and Harikumar, K. B. (2009). "Potential therapeutic effects of curcumin, the anti-inflammatory agent, against neurodegenerative, cardiovascular, pulmonary, metabolic, autoimmune and neoplastic diseases." *The International Journal of Biochemistry & Cell Biology*, Vol. 41, No. 1, pp. 40-59.

[12] Weber, W. M., Hunsaker, L. A., Abcouwer, S.F., Deck, L.M. and Vander Jagt, D. L. (2005). "Antioxidant activities of curcumin and related enones." *Bioorganic & Medicinal Chemistry*, Vol. 13, No. 11, pp. 3811-3820.

[13] Dikshit, M., Rastogi, L., Shukla, R. and Srimal, R.C. (1995). "Prevention of ischaemia-induced biochemical changes by curcumin & quinidine in the cat heart." *The Indian Journal of Medical Research*, Vol. 101, pp. 31-35.

[14] Nirmala, C. and Puvanakrishnan, R. (1996). "Protective role of curcumin against isoproterenol induced myocardial infarction in rats." *Molecular and Cellular Biochemistry*, Vol. 159, No. 2, pp. 85-93.

[15] Venkatesan, N. (1998). "Curcumin attenuation of acute adriamycin myocardial toxicity in rats." *British Journal of Pharmacology*, Vo. 124, No. 3, pp. 425-427.

[16] Rao, C. V., Rivenson, A., Simi, B. and Reddy, B. S. (1995). "Chemoprevention of colon carcinogenesis by dietary curcumin, a naturally occurring plant phenolic compound." *Cancer Research*, Vol. 55, No. 2, pp. 259-266.

[17] Kuttan, R., Sudheeran, P. C., and Josph, C. D. (1987). "Turmeric and curcumin as topical agents in cancer therapy." *Tumori Journal*, Vol. 73, No. 1, pp. 29-31.

[18] Shishodia, S., Chaturvedi, M.M. and Aggarwal, B. B. (2007). "Role of curcumin in cancer therapy." *Current Problems in Cancer*, Vol. 31, No. 4, pp. 243-305.

[19] Tomren, M.A., Masson, M., Loftsson, T. and Tønnesen, H. H. (2007). "Studies on curcumin and curcuminoids: XXXI. Symmetric and asymmetric curcuminoids: stability, activity and complexation with cyclodextrin." *International Journal of Pharmaceutics*, Vol. 338, No. 1-2, 27-34.

[20] Kurien, B. T., Singh, A., Matsumoto, H. and Scofield, R. H. (2007). "Improving the solubility and pharmacological efficacy of curcumin by heat treatment." *Assay and Drug Development Technologies*, Vol. 5, No. 4, pp. 567-576.

[21] Nagavarma, B. V. N., Yadav, H. K., Ayaz, A., Vasudha, L. S., and Shivakumar, H. G. (2012). "Different techniques for preparation of polymeric nanoparticles-a review." *Asian Journal of Pharmaceutical and Clinical Research*, *5*(3), 16-23.

[22] Zambaux, M. F., Bonneaux, F., Gref, R., Maincent, P., Dellacherie, E., Alonso, M. J. and Vigneron, C. (1998). "Influence of experimental parameters on the characteristics of poly (lactic acid) nanoparticles prepared by a double emulsion method." *Journal of Controlled Release*, Vol. 50, No. 1-3, pp. 31-40.

[23] Jain, R. A. (2000). "The manufacturing techniques of various drug loaded biodegradable poly (lactide-co-glycolide) (PLGA) devices." *Biomaterials*, Vol. 21, No. 23, pp. 2475-2490.

[24] McCarron, P.A., Donnelly, R.F. and Marouf, W. (2006). "Celecoxib-loaded poly (D, L-lactide-co-glycolide) nanoparticles prepared using a novel and controllable combination of diffusion and emulsification steps as part of the salting-out procedure." *Journal of Microencapsulation*, Vol. 23, No. 5, pp. 480-498.

[25] Soppimath, K. S., Aminabhavi, T. M., Kulkarni, A. R. and Rudzinski, W. E. (2001). "Biodegradable polymeric nanoparticles as drug delivery devices." *Journal of Controlled Release*, Vol. 70, No. 1-2, pp. 1-20.

[26] Scholes, P. D., Coombes, A. G. A., Illum, L., Daviz, S. S., Vert, M. and Davies, M.C. (1993). "The preparation of sub-200 nm poly (lactide-co-glycolide) microspheres for site-specific drug delivery." *Journal of Controlled Release*, Vol. 25, No. 1-2, pp. 145-153.

[27] Rietveld, I. B., Kobayashi, K., Yamada, H. and Matsushige, K. (2006). "Electrospray deposition, model, and experiment: Toward general control of film morphology." *The Journal of Physical Chemistry B*, Vol. 110, No. 46, pp. 23351-23364.

[28] Bagheri-Tar, F., Sahimi, M. and Tsotsis, T. T. (2007). "Preparation of polyetherimide nanoparticles by an electrospray technique." *Industrial & Engineering Chemistry Research*, Vol. 46, No. 10, pp. 3348-3357.

[29] Jaworek, A. (2007). "Micro-and nanoparticle production by electrospraying." *Powder Technology*, Vol. 176, No. 1, pp. 18-35.

[30] Jaworek, A. T. S. A., and Sobczyk, A. T. (2008). "Electrospraying route to nanotechnology: An overview." *Journal of Electrostatics*, Vol. 66, No. 3-4, pp. 197-219.

[31] Chakraborty, S., Liao, I. C., Adler, A. and Leong, K.W. (2009). "Electrohydrodynamics: a facile technique to fabricate drug delivery systems." *Advanced Drug Delivery Reviews*, Vol. 61, No. 12, pp. 1043-1054.

[32] Jaworek, A. and Krupa, A. (1999). "Classification of the modes of EHD spraying." *Journal of Aerosol Science*, Vol. 30, No. 7, pp. 873-893.

[33] Zhang, S. and Kawakami, K. (2010). "One-step preparation of chitosan solid nanoparticles by electrospray deposition." *International Journal of Pharmaceutics*, Vol. 397, No. 1-2, pp. 211-217.

[34] Hogan Jr, C. J., Yun, K. M., Chen, D. R., Lenggoro, I. W., Biswas, P. and Okuyama, K. (2007). "Controlled size polymer particle production via electrohydrodynamic atomization." *Colloids and Surfaces A: Physicochemical and Engineering Aspects*, Vol. 311, No. 1-3, pp. 67-76.

[35] Ijsebaert, J. C., Geerse, K. B., Marijnissen, J. C., Lammers, J. W. J., and Zanen, P. (2001). "Electrohydrodynamic atomization of drug solutions for inhalation purposes." *Journal of Applied Physiology*, Vol. 91, No. 6, pp. 2735-2741.

[36] Zarchi, A. A. K., Abbasi, S., Faramarzi, M. A., Gilani, K., Ghazi-Khansari, M. and Amani, A. (2015). "Development and optimization of N-Acetylcysteine-loaded poly (lactic-co-glycolic acid) nanoparticles by electrospray." *International Journal of Biological Macromolecules*, Vol. 72, pp. 764-770.

[37] Liu, J., Xu, L., Liu, C., Zhang, D., Wang, S., Deng, Z. and Ma, J. (2012). "Preparation and characterization of cationic curcumin nanoparticles for improvement of cellular uptake." *Carbohydrate Polymers*, Vol. 90, No. 1, pp. 16-22.

[38] Steyaert, I., Van der Schueren, L., Rahier, H. and De Clerck, K. (2012). "An alternative solvent system for blend electrospinning of polycaprolactone/chitosan nanofibres." *Macromolecular Symposia*. Vol. 321, No. 1, pp. 71-75.

[39] Van der Schueren, L., Steyaert, I., De Schoenmaker, B. and De Clerck, K. (2012). "Polycaprolactone/chitosan blend nanofibres electrospun from an acetic acid/formic acid solvent system." *Carbohydrate Polymers*, Vol. 88, No. 4, pp. 1221-1226.

[40] Chawla, J. S. and Amiji, M. M. (2002). "Biodegradable poly (ε-caprolactone) nanoparticles for tumor-targeted delivery of tamoxifen." *International Journal of Pharmaceutics*, Vol. 249, No. 1, pp. 127-138.

[41] Ilium, L. (1998). "Chitosan and its use as a pharmaceutical excipient." *Pharmaceutical Research*, Vol. 15, No. 9, pp. 1326-1331.

[42] Rinaudo, M. (2006). "Chitin and chitosan: properties and applications. *Progress in Polymer Science*." Vol. 31, No. 7, pp. 603-632.

[43] Wu, L., Li, H., Li, S., Li, X., Yuan, X., Li, X. and Zhang, Y. (2010). "Composite fibrous membranes of PLGA and chitosan prepared by coelectrospinning and coaxial electrospinning." *Journal of Biomedical Materials Research Part A: An Official Journal of The Society for Biomaterials, The Japanese Society for Biomaterials, and The Australian Society for Biomaterials and the Korean Society for Biomaterials*, Vol. 92, No. 2, pp. 563-574.

[44] Hartman, R. P. A., Brunner, D. J., Camelot, D. M. A., Marijnissen, J. C. M., and Scarlett, B. (2000). "Jet break-up in electrohydrodynamic atomization in the cone-jet mode." *Journal of Aerosol Science*, Vol. 31, No. 1, pp. 65-95.

[45] Ganan-Calvo, A. M., Davila, J., and Barrero, A. (1997). "Current and droplet size in the electrospraying of liquids. Scaling laws." *Journal of Aerosol Science*, Vol. 28, No. 2, pp. 249-275.

[46] Enayati, M., Ahmad, Z., Stride, E., and Edirisinghe, M. (2010). "Size mapping of electric field-assisted production of polycaprolactone particles." *Journal of The Royal Society Interface*, Vol. 7 No. Suppl 4, pp. S393-S402.

[47] Lee, Y. H., Mei, F., Bai, M. Y., Zhao, S., and Chen, D. R. (2010). "Release profile characteristics of biodegradable-polymer-coated drug particles fabricated by dual-capillary electrospray." *Journal of Controlled Release*, Vol. 145, No. 1, pp. 58-65.

[48] Mohan, P. K., Sreelakshmi, G., Muraleedharan, C. V. and Joseph, R. (2012). "Water soluble complexes of curcumin with cyclodextrins: Characterization by FT-Raman spectroscopy." *Vibrational Spectroscopy*, Vol. 62, pp. 77-84.

[49] Elzein, T., Nasser-Eddine, M., Delaite, C., Bistac, S. and Dumas, P. (2004). "FTIR study of polycaprolactone chain organization at interfaces." *Journal of Colloid and Interface Science*, Vol. 273, No. 2, pp. 381-387.

[50] Jayasree, A., Sasidharan, S., Koyakutty, M., Nair, S., and Menon, D. (2011). "Mannosylated chitosan-zinc sulphide nanocrystals as fluorescent bioprobes for targeted cancer imaging." *Carbohydrate Polymers*, Vol. 85, No. 1, pp. 37-43.